Automatic lesion detection in capsule endoscopy based on color saliency: closer to an essential adjunct for reviewing software

Dimitris K. Iakovidis, MSc, PhD,[1] Anastasios Koulaouzidis, MD, FRCPE[2]

Lamia, Greece; Edinburgh, United Kingdom

Background: The advent of wireless capsule endoscopy (WCE) has revolutionized the diagnostic approach to small-bowel disease. However, the task of reviewing WCE video sequences is laborious and time-consuming; software tools offering automated video analysis would enable a timelier and potentially a more accurate diagnosis.

Objective: To assess the validity of innovative, automatic lesion-detection software in WCE.

Design/intervention: A color feature-based pattern recognition methodology was devised and applied to the aforementioned image group.

Setting: This study was performed at the Royal Infirmary of Edinburgh, United Kingdom, and the Technological Educational Institute of Central Greece, Lamia, Greece.

Materials: A total of 137 deidentified WCE single images, 77 showing pathology and 60 normal images.

Results: The proposed methodology, unlike state-of-the-art approaches, is capable of detecting several different types of lesions. The average performance, in terms of the area under the receiver-operating characteristic curve, reached $89.2 \pm 0.9\%$. The best average performance was obtained for angiectasias ($97.5 \pm 2.4\%$) and nodular lymphangiectasias ($96.3 \pm 3.6\%$).

Limitations: Single expert for annotation of pathologies, single type of WCE model, use of single images instead of entire WCE videos.

Conclusion: A simple, yet effective, approach allowing automatic detection of all types of abnormalities in capsule endoscopy is presented. Based on color pattern recognition, it outperforms previous state-of-the-art approaches. Moreover, it is robust in the presence of luminal contents and is capable of detecting even very small lesions.

Wireless capsule endoscopy (WCE) established a new era in the investigation and diagnosis of small-bowel diseases. Once a capsule endoscope is ingested, it begins to transmit color images, resulting in a large volume of imaging data.[1] The average WCE analysis requires 45 to 90 minutes of intense focus and attention.[2] Current software for WCE video analysis enables automatic detection of only a few kinds of abnormalities. A computational method enabling the detection of a broader spectrum of pathologies is highly desirable.

A state-of-the-art method, influenced by this concept, is capable of automatically selecting representative frames,

TABLE 1. Composition of the experimental images dataset

Type of pathology	No. of images	Minimal size, % of pixels (absolute no. of pixels)	Maximal size, % of pixels (absolute no. of pixels)
Angiectasias			
P0	9	0.1 (152)	4.5 (4576)
P1	9	0.7 (675)	3.7 (3796)
P2	9	2.2 (2219)	11.9 (12,169)
Intraluminal hemorrhage	5	5.4 (5550)	55.2 (56,481)
Aphthae	5	0.3 (324)	27.2 (27,881)
Ulcers	9	0.9 (939)	24.5 (25,133)
Stenoses	6	18.4 (18,843)	42.8 (43,848)
Villous edema	2	12.7 (13,040)	81.0 (82,896)
Nodular lymphangiectasias	9	2.3 (2326)	10.6 (10,875)
Chylous cysts	8	7.9 (8109)	37.4 (38,323)
Polyps	6	18.7 (19,178)	68.8 (69,600)
Normal/no pathology	60	–	–
Total	137	0.1 (152)	81.0 (82,896)

Take-Home Message

- Review of capsule video sequences is a laborious task; software tools that offer automated video analysis would enable a timelier diagnosis.
- A color feature–based pattern recognition methodology is capable of automatic detection of several different types of lesions. It outperforms previous state-of-the-art approaches and exhibits robustness in the presence of luminal content while it is capable of detecting even the very small lesions.

selected subset of 137 images (10%). Hence, the experimental dataset included 77 images with abnormal findings and 60 images without visible abnormalities, including intestinal content such as bubbles and/or luminal debris or opaque fluid, to simulate clinical practice outcomes (Table 1).

For each abnormality, a graphic annotation was constructed using Ratsnake (Fig. 1B), publicly available software for image annotation.[5] Annotated images were exported as masks, ie, black-and-white frames in which any pathology is depicted as white area on a black background (Fig. 1C). Abnormalities included in this dataset range from very small (152 pixels; 0.1% of the image) to very large (82,986 pixels; 81% of the image). The total number of pixels corresponding to pathologies is 1,096,020 (7.81% of the total $137 \times 320 \times 320 = 1.4 \times 10^7$ pixels). Disjoint subsets of the annotated images are used as a criterion standard for the training of the machine learning–based classification algorithm and for the evaluation of the proposed methodology. The entire annotated dataset is available online (ftp://data:data@innovation.teilam.gr).

Pattern recognition methodology

The proposed methodology consists of the following 4 steps (Fig. 2).

Color transformation. Color representation in digital devices is typically based on the red, green, blue model, in which any color can be composed by different proportions of red, green and blue. More perceptual representations can be obtained by separating intensity from chromatic image components. To this end, the colors of WCE images are transformed to CIE-Lab representation, where component L describes the lightness of colors, and a and b describe their chromaticities (Fig. 2A, B).[7]

Salient point selection. Bay et al[8] proposed the speeded-up robust feature extraction algorithm for automatic selection of salient points in digital images. This algorithm is based on changes observed in image intensities at multiple scales. Considering the importance of color in digestive endoscopy,[9] the speeded-up robust feature is modified here to select points based on a chromatic rather than an image-intensity component. The salient point selection (SPS) algorithm includes a threshold (T) parameter

thus significantly reducing reviewing time.[3,4] However, it has a high complexity and does not directly address the issue of automated lesion detection.[5] A methodology designed for the detection of a wide variety of lesions, regardless of their type or size, should be able to overcome such limitations. Toward this direction, the simple approach proposed in this article is based solely on color information extracted from visually salient points of WCE video frames.

METHODS

Images

A total of 1370 representative images were obtained from 252 WCE procedures with MiroCam (IntroMedic Co, Seoul, South Korea) at the Royal Infirmary of Edinburgh. The MiroCam capsule endoscope has a frame rate of 3 frames per second and an image resolution of 320×320 pixels. An expert WCE reviewer (A.K.) categorized these images into normal and pathological. Thereafter, based on a standard terminology[6] the lesions were classified into 4 categories: vascular, inflammatory, lymphangiectatic, and polypoid. The performance of the proposed methodology was assessed on a randomly
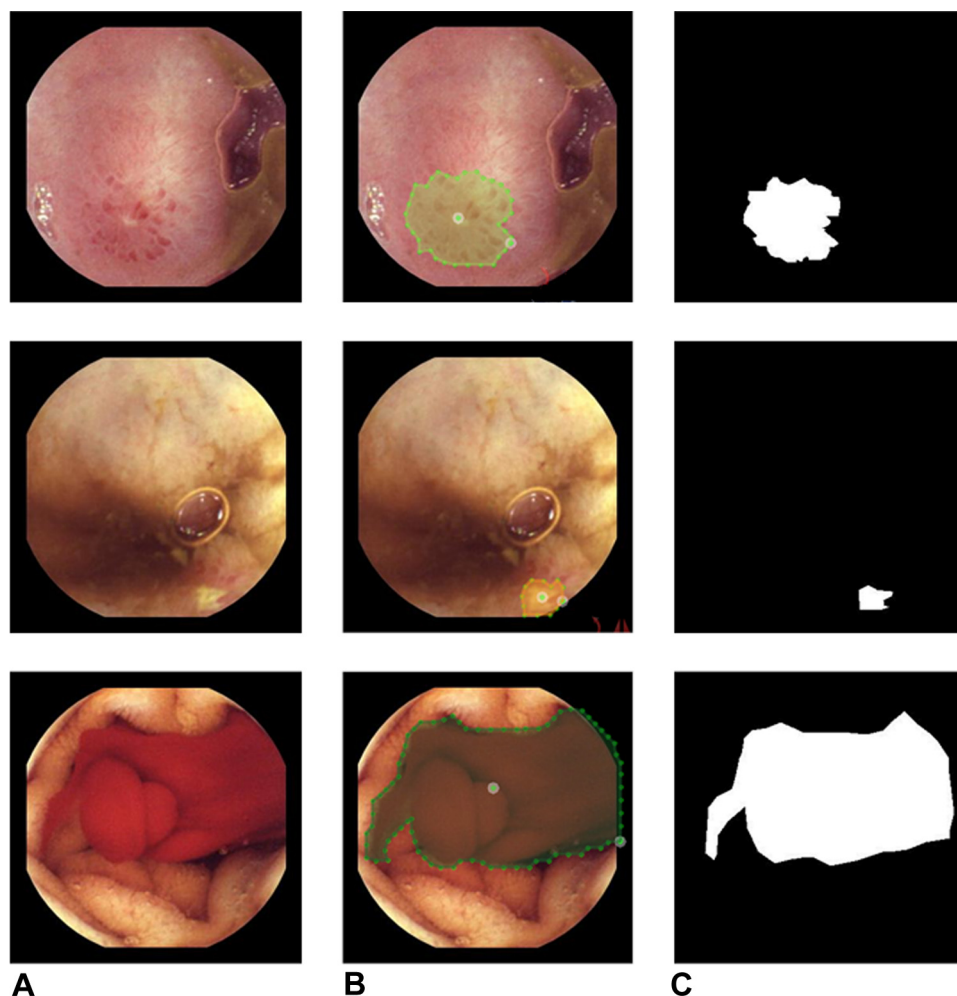
Figure 1. Construction of criterion-standard image annotations. **A**, Original images of an aphtha (*first row*), a small mucosal ulcer (*second row*), and intraluminal (third row). **B**, Graphic annotations made using the Ratsnake annotation tool 10. **C**, Masks, ie, black-and-white images used as a criterion standard (black corresponds to normal, and white corresponds to abnormal regions in each frame).

that controls its sensitivity; as T increases, fewer salient points are selected (Fig. 2C).

Feature extraction. For each salient point, the following numerical features of image content are considered (Fig. 2D): (1) The value of each color component, enabling a pixel-level description of the image; (2) the minimal and maximal values of each color component calculated over a square neighborhood of pixels around the salient point, ie, in a CIE Lab color model, a set of 6 values is calculated (minimal and maximal values for each CIE Lab component).

Some lesions (eg, mucosal ulcers) may have similar color with the intestinal content; hence, by considering the color around a point of interest, the lesions are usually discriminated. This set of features constitutes a feature vector (Fig. 2E).

Classification. The extracted feature vectors are classified into normal and abnormal, by a support vector machine learning algorithm[10] (Fig. 2F).

Methodology evaluation

A 2-phase experimental evaluation was performed. Phase 1 determined the optimal color component and parameter T for 100% detection of the abnormalities by using a minimal number of salient points. The SPS algorithm was applied to all CIE Lab components and on chromatic components of 4 other color models previously considered for WCE video analysis.

Phase 2 investigated the classification of the salient points into normal and abnormal classes. The experiments were performed by the support vector machine classifier by using a radial basis function kernel, which has resulted in best performance in previous studies,[11,12] and it is well-known for its learning capacity.[10] To limit the bias, classification performance was evaluated by using the 10-fold cross-validation strategy and averaging of the results,[13] ie, the dataset was randomly partitioned into 10 equally sized disjoint subsets, a single subset was retained as the validation data for testing the
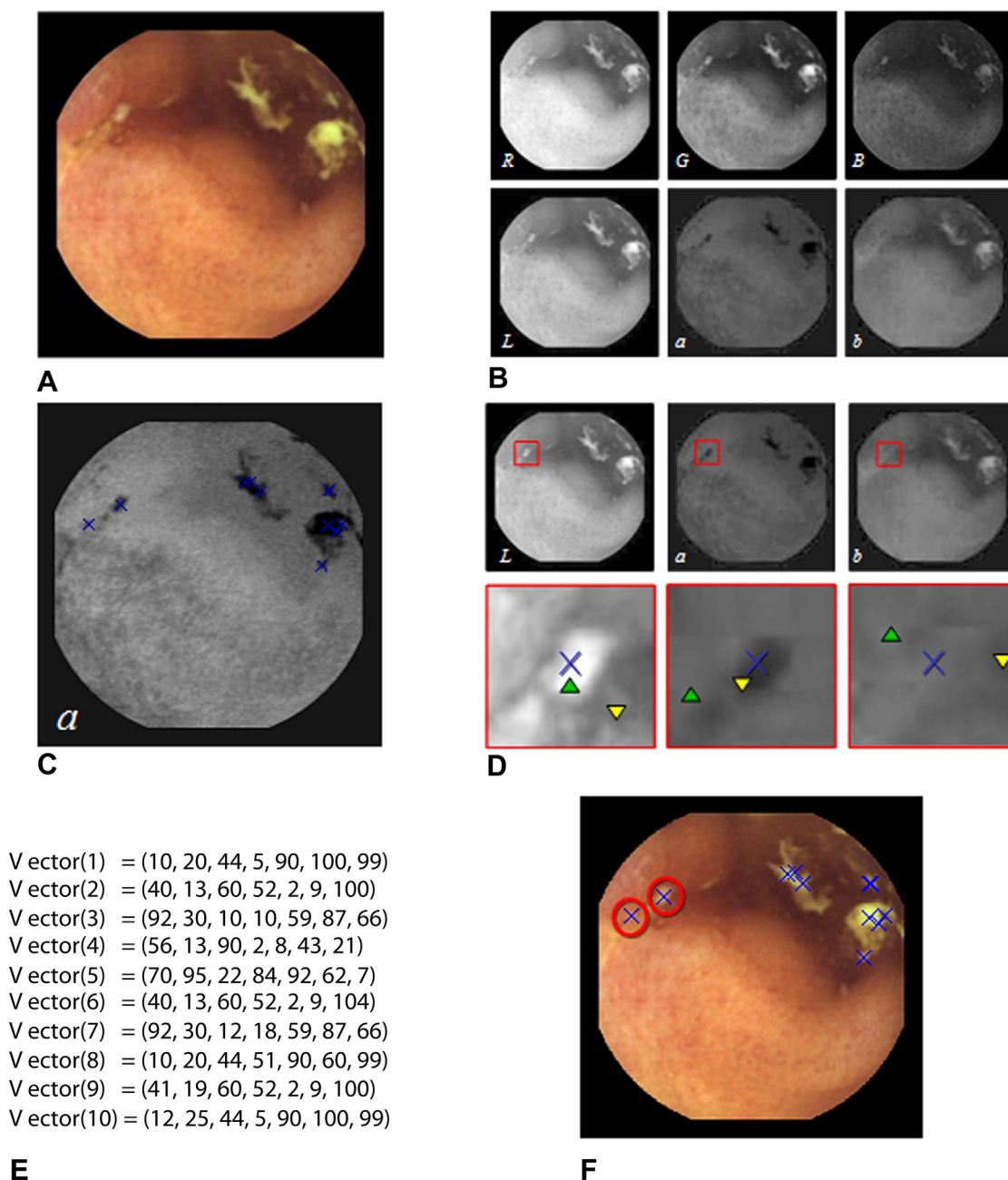
$$V\ ector(1)\ = (10, 20, 44, 5, 90, 100, 99)$$
$$V\ ector(2)\ = (40, 13, 60, 52, 2, 9, 100)$$
$$V\ ector(3)\ = (92, 30, 10, 10, 59, 87, 66)$$
$$V\ ector(4)\ = (56, 13, 90, 2, 8, 43, 21)$$
$$V\ ector(5)\ = (70, 95, 22, 84, 92, 62, 7)$$
$$V\ ector(6)\ = (40, 13, 60, 52, 2, 9, 104)$$
$$V\ ector(7)\ = (92, 30, 12, 18, 59, 87, 66)$$
$$V\ ector(8)\ = (10, 20, 44, 51, 90, 60, 99)$$
$$V\ ector(9)\ = (41, 19, 60, 52, 2, 9, 100)$$
$$V\ ector(10) = (12, 25, 44, 5, 90, 100, 99)$$

Figure 2. Outline of the proposed methodology. **A**, Original red, green, blue (RGB) wireless capsule endoscopy image. **B**, Color transformation of RGB image components (*first row*) to CIE Lab image components (*second row*). **C**, Salient point selection from component a; the salient points are indicated with *cross marks*. **D**, Feature extraction from each salient point (1 salient point is used as an example). A square neighborhood of pixels is isolated per component (*first row*). Within the neighborhood (*second row*), the following are considered features: (1) the value of each L, a, b component from the central pixel, indicated by *cross marks*; (2) the minimal and maximal values from each neighborhood indicated by *upright triangles* and *inverted triangles*, respectively. **E**, Example feature vectors composed of features extracted from each of the 10 salient points. **F**, The feature vectors and therefore the respective salient points are classified into normal and abnormal (indicated by *circled areas*).

model, and the remaining 9 subsets were used as training data.

Statistical analysis

Statistical analysis was performed with MATLAB software (MathWorks, Natick, Mass).[14] The classification was assessed by receiver-operating characteristic analysis and quantified by the area under receiver-operating characteristic (AUC). The AUC represents an intuitive performance measure even when the datasets are characterized by imbalanced class distributions.[15] An AUC close to 100% signifies a near-perfect sample classification, whereas
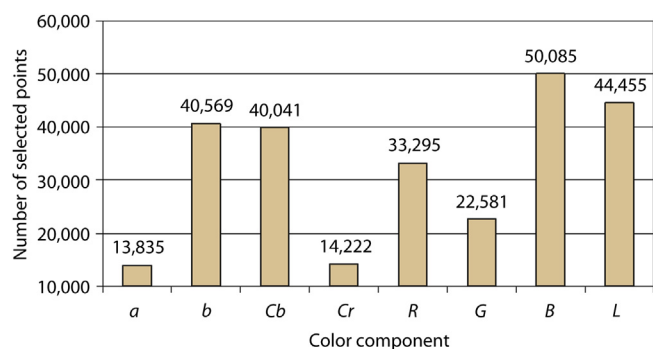
Figure 3. The number of salient points selected by using components from various color models. Representative color models include hue saturation, value (HSV), CIE Lab, Luminance Y, Chroma: Blue, Chroma: Red (YCbCr), where intensity is represented by brightness value, lightness (L), and luma components, and chromatic information is represented by hue, color opponents (a, b), blue difference (Cb), and red (R) difference components, respectively. B, blue; G, green.

an AUC close to 50% suggests a random classification. A 2-tailed P value $<.05$ was considered as statistically significant.

RESULTS

Phase 1: SPS

An abnormality was considered detected if at least 1 of the salient points selected by the SPS algorithm belonged to this abnormality. To determine the optimal color component, a range of thresholds was tested (100-2500). The results are illustrated in Figure 3. The lesion detection problem can be significantly narrowed (99.90% pixel reduction) without abnormality misses by using the chromatic component a of CIE Lab (T = 2000). Representative examples of automatically selected salient points are illustrated in Figure 4.

Phase 2: classification

Because of the results of phase 1, the CIE Lab color model was chosen. The proposed methodology provided a higher average AUC compared with baseline (by using only CIE Lab color components, without minimal-maximal features) and state-of-the-art approaches[12,16] (Fig. 5). The respective average accuracy (ie,, the percentage of correctly classified samples) is 94.0 ± 0.5%, and the average sensitivity and specificity are 95.4 ± 0.6% and 82.9 ± 1.7%, respectively.

To investigate which classes of pathologies are better discriminated from normal samples, additional classification experiments were performed by following the same strategy. The results are illustrated in Figure 6. All pathologies are generally well detected, with best average performance obtained for angiectasias P1 (ie, lesions of intermediate probability of bleeding).
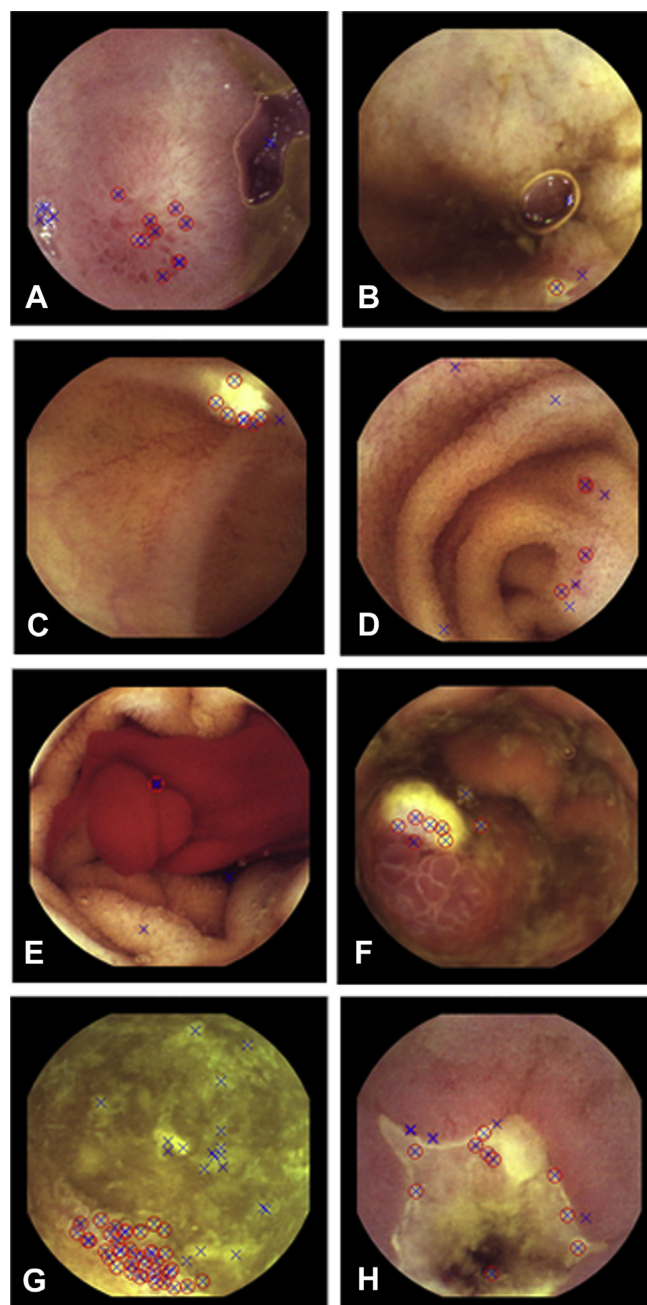

Figure 4. Automatically selected salient points by using the chromatic component a of CIE Lab color model. The selected points are indicated by *cross marks* and those corresponding to abnormalities (according to the criterion standard annotations) are indicated by *circular marks*. Even very small lesions remain well detected. **A**, Aphtha. **B**, Ulcer. **C**, Nodular lymphangiectasia. **D**, Angiectasia. **E**, Hemorrhage. **F**, Polyp. **G**, Villous edema. **H**, Stenosis.

DISCUSSION

We present an efficient methodology that aims to be used as a supportive tool for automatic detection of a broad spectrum of abnormalities in WCE, considering color as a discriminative feature of importance.[9] The results
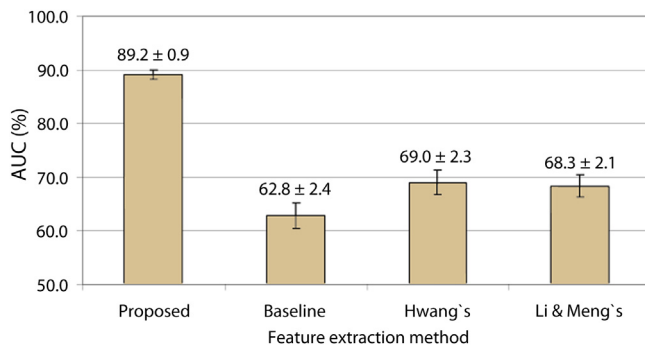
Figure 5. Classification results obtained by using the proposed methodology in comparison with the results obtained with other methodologies. The error bars represent ±SD. *AUC*, area under the receiver-operating characteristic curve.

confirm that it can be more accurate than state-of-the-art approaches, while being robust in the presence of luminal content and capable of detecting small lesions.

WCE has proved superior to other modalities for small-bowel investigation. However, the detection rate of clinically significant findings is rather low and likely not influenced by increasing reviewer's experience.[17] The analysis of endoscopic videos has attracted the interest of researchers since the early 2000s.[18] The Suspected Blood Indicator (Given Imaging Ltd, Yokneam, Israel) is a commercially available solution, but it can only be used as supportive tool for bleeding detection, and it has a suboptimal performance.[2] Other state-of-the-art abnormality detection methods in WCE, with their results, are summarized in Table 2. Only a few of them, unlike our method, address the detection of more than a single type of abnormality.[19,24,25]

TABLE 2. Recent studies on computational methods for abnormality detection: the best results are presented in the way in which they are reported in these studies

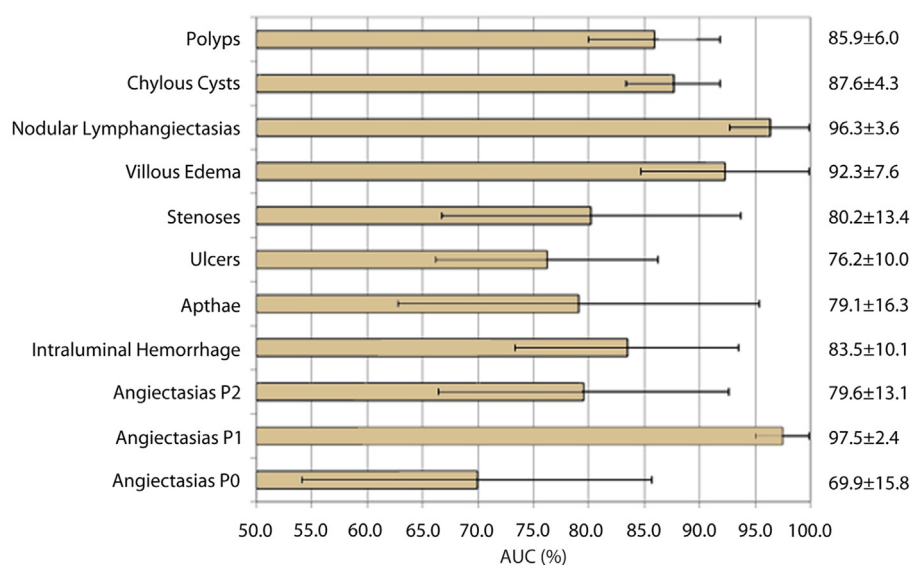| Study	Abnormality	Best results Accuracy, %
Li and Meng,[19] 2009	Hemorrhage	91.8
Lv et al,[20] 2011	Hemorrhage	97.9
Charisis et al,[21] 2013	Ulcers	91.1
Yu et al,[22] 2012	Ulcers	89.5
Kumar et al,[23] 2012	CD lesions	92.0
Li and Meng,[11] 2012	Polyps	91.6
Hwang,[12] 2011	Polyps	89.5
		Sensitivity/specificity
Li and Meng,[11] 2012	Polyps	84.7 ± 1.5/82.3 ± 1.9
Yu et al,[22] 2012	Ulcers	99.2/80.0
Karargyris and Bourbakis,[24] 2011	Polyps	96.2/70.2
	Ulcers	75.0/73.3
Szczypinski et al,[25] 2014	Hemorrhage	100.0/99.0
	Ulcers	83.0/94.0

CD, Crohn's disease.

Figure 6. Classification results per pathology obtained by using the proposed methodology. The error bars represent ±SD. *AUC*, area under the receiver-operating characteristic curve.

Limitations of this study include the use of 1 expert to create criterion-standard graphic annotations of abnormalities, the use of a single type of capsule endoscope model, and a dataset limited to single video frames instead of whole WCE videos. However, this was a compromise for obtaining graphic annotations of all included abnormalities manually. Regarding this issue, one would argue that if the algorithm performs so well with single frames, it is expected to offer similar results in WCE videos, where an abnormality is usually depicted in more than 1 frame.

REFERENCES

1. Koulaouzidis A, Rondonotti E, Karargyris A. Small-bowel capsule endoscopy: a ten-point contemporary review. World J Gastroenterol 2013;19: 3726.
2. Lo SK. How should we do capsule reading? Tech Gastrointest Endosc 2006;8:146-8.
3. Iakovidis DK, Tsevas S, Polydorou A. Reduction of capsule endoscopy reading times by unsupervised image mining. Comput Med Imaging Graph 2010;34:471-8.
4. Kanaris I, Tsevas S, Maglogiannis I, Iakovidis DK. Enabling distributed summarization of wireless capsule endoscopy video. In: Imaging Systems and Techniques (IST), 2010 IEEE International Conference on: IEEE; 2010. p. 17-21.
5. Iakovidis D, Goudas T, Smailis C, et al. Ratsnake: a versatile image annotation tool with application to computer-aided diagnosis. Sci World J 2014;2014:286856.
6. Korman L, Delvaux M, Gay G, et al. Capsule endoscopy structured terminology (CEST): proposal of a standardized and structured terminology for reporting capsule endoscopy procedures. Endoscopy 2005;37: 951-9.
7. Wyszecki G, Stiles WS. Color science. Vol. 8. New York (NY): Wiley; 1982.
8. Bay H, Ess A, Tuytelaars T, et al. Speeded-up robust features (SURF). Comput Vision Image Understand 2008;110:346-59.
9. Tanaka M, Kidoh Y, Kamei M, et al. A new instrument for measurement of gastrointestinal mucosal color. Dig Endosc 1996;8:139-46.
10. Burges CJ. A tutorial on support vector machines for pattern recognition. Data Mining Knowledge Discovery 1998;2:121-67.
11. Li B, Meng MQH. Automatic polyp detection for wireless capsule endoscopy images. Expert Syst Applications 2012;39:10952-8.
12. Hwang S. Bag-of-visual-words approach to abnormal image detection in wireless capsule endoscopy videos. In: Advances in visual computing. New York (NY): Springer; 2011. p. 320-7.
13. Airola A, Pahikkala T, Waegeman W, et al. An experimental comparison of cross-validation techniques for estimating the area under the ROC curve. Comput Stat Data Anal 2011;55:1828-44.
14. Blanchet G, Charbit M. Digital signal and image processing using Matlab. Vol. 666. Hoboken (NJ): John Wiley & Sons; 2010.
15. Fawcett T. An introduction to ROC analysis. Pattern Recognition Lett 2006;27:861-74.
16. Li BP, Meng MQH. Comparison of several texture features for tumor detection in CE images. J Med Syst 2012;36:2463-9.
17. Zheng Y, Hawkins L, Wolff J, et al. Detection of lesions during capsule endoscopy: physician performance is disappointing. Am J Gastroenterol 2012;107:554-60.
18. Karkanis SA, Iakovidis DK, Karras D, et al. Detection of lesions in endoscopic video using textural descriptors on wavelet domain supported by artificial neural network architectures. 2001. Proceedings of the 2001 International Conference on Image Processing, vol. 2. IEEE; 2001. p. 833-6.
19. Li B, Meng MH. Computer-aided detection of bleeding regions for capsule endoscopy images. IEEE Trans Biomed Eng 2009;56:1032-9.
20. Lv G, Yan G, Wang Z. Bleeding detection in wireless capsule endoscopy images based on color invariants and spatial pyramids using support vector machines. In: Engineering in Medicine and Biology Society, 2011 Annual International Conference of the IEEE. IEEE; 2011. p. 6643-6.
21. Charisis VS, Katsimerou C, Hadjileontiadis LJ, et al. Computer-aided capsule endoscopy images evaluation based on color rotation and texture features: an educational tool to physicians. In: IEEE 26th International Symposium on Computer-Based Medical Systems (CBMS). IEEE; 2013. p. 203-8.
22. Yu L, Yuen PC, Lai J. Ulcer detection in wireless capsule endoscopy images. In: 21st International Conference on Pattern Recognition (ICPR). IEEE; 2012. p. 45-8.
23. Kumar R, Zhao Q, Seshamani S, et al. Assessment of Crohn's disease lesions in wireless capsule endoscopy images. IEEE Trans Biomed Eng 2012;59:355-62.
24. Karargyris A, Bourbakis N. Detection of small bowel polyps and ulcers in wireless capsule endoscopy videos. IEEE Trans Biomed Eng 2011;58: 2777-86.
25. Szczypinski P, Klepaczko A, Pazurek M, et al. Texture and color based image segmentation and pathology detection in capsule endoscopy videos. Comput Methods Programs Biomed 2014;113:396-411.